Dielectric relaxations in PVDF/BaTiO₃ nanocomposites

C. V. Chanmal, J. P. Jog[*]

Polymer Science and Engineering Division, National Chemical Laboratory, Dr. Homi Bhabha Road, Pashan, Pune-411008, India

Abstract. The present work aims at the study of molecular relaxations in PVDF/BaTiO₃ nanocomposites using broadband dielectric spectroscopy. The nanocomposites of PVDF with BaTiO₃ (10–30% by wt%) are prepared using simple melt mixing method. In dielectric permittivity study, two relaxation processes are identified corresponding to the crystalline, glass transition in the PVDF/BaTiO₃ nanocomposites. The peaks shift to higher frequencies as the temperature is increased. Electric modulus formalism is used to analyze the dielectric relaxations to overcome the conductivity effects at low frequencies. In M'' spectra two peaks are observed only at high temperature and low frequency whereas a single relaxation peak appears at low temperatures. The single relaxation peak appearing at low temperatures is the α_c relaxation attributed to crystalline chain relaxation in PVDF and the second relaxation peak which appears only at high temperatures and at a frequency lower than α_c relaxation is identified as MWS relaxation. The temperature dependence of α_c relaxation and MWS relaxation follows Arrhenius type behavior.

Keywords: nanocomposites, dielectric spectroscopy, MWS relaxation, interfacial polarization

1. Introduction

Nanocomposites of electroactive ceramics and a ferroelectric polymer are very attractive for many applications as their properties can be easily tailored to suit particular performance requirements [1]. In these nanocomposites, the final properties depend essentially on parameters such as grain size of ceramic, method of preparation of composites and on the dispersion of the ceramic particles into the polymer matrix [2–5]. PVDF is semicrystalline polymer with pyro and piezoelectric properties. Its high permittivity and relatively low dissipation factor made it a potential candidate to useful in many applications [6, 7]. The piezoelectric and pyroelectric properties of PVDF have led for intensive technological applications. Piezoelectric polymers have advantage over piezoelectric ceramics for certain applications wherein acoustic impedance similar to that of water or living tissue is required [8]. Due to

this reason PVDF is increasingly used for medical and industrial applications.

Although, there are several techniques to understand dynamics in polymer nanocomposites, dielectric spectroscopy is a well established tool for materials characterization [9, 10]. The magnitude and frequency location of the energy absorption associated with various processes depends critically on physical and chemical nature of the material [11].

In this article, we present the results of relaxations in PVDF/BaTiO₃ nanocomposites prepared by melt compounding technique. Although there have been few reports on PVDF/BaTiO₃ composites with high loading of BaTiO₃ (upto 50% by volume) the relaxations in this nanocomposites were not studied [12, 13]. In the present work, relaxations in PVDF/BaTiO₃ at low BaTiO₃ content i.e. upto 11.5% by volume are investigated using dielectric spec-

---
[*]Corresponding author, e-mail: jp.jog@ncl.res.in

troscopy over a temperature range from 30 to 150°C.

2. Experimental

2.1. Materials

PVDF grade, Solef 1008 (with weight-average molecular weight of $100 \cdot 10^3$ g/mol) procured by Solvay Belgium is used for this study. $BaTiO_3$ nanoparticles (formula weight = 233.24) of more than 99% purity are procured from Aldrich chemicals. The average diameter of the particle is around 30–50 nm.

2.2. Melt processing of PVDF/BaTiO₃ nanocomposites

The nanocomposites of PVDF with various weight percent of $BaTiO_3$ (10, 20 & 30% wt/wt) are processed via melt mixing in Thermo Haake Polylab batch mixer at 200°C, with 60 rpm for 5 minutes. The films of uniform thickness are compression molded at 200°C under 5-ton pressure using Carver Press (Germany). The thickness of the films is about 0.4 to 0.5 mm.

2.3. Characterization techniques

2.3.1. Scanning electron microscopy (SEM)

The dispersion of $BaTiO_3$ nanoparticles in the polymer matrix is determined from the morphology of fractured surfaces of PVDF/$BaTiO_3$ nanocomposites using Leica-440 scanning electron microscope. Cryo-fractured films are used for this purpose and fractured surfaces are sputtered by gold to avoid overcharging.

2.3.2. Dielectric relaxation spectroscopy (DRS)

Complex dielectric permittivity measurement of PVDF and PVDF/$BaTiO_3$ nanocomposites is done using Novocontrol broadband dielectric spectrometer with the ZGS active sample cell equipped with temperature controller and WinFit software for data analysis. The dielectric response of material in the frequency ranging from 10 MHz to 0.01 Hz over the temperature range of 30 to 150°C is measured by placing sample between two 20 mm gold plated electrodes. Quick drying silver paste is used to ensure good electrical contact.

3. Results and discussion

3.1. Morphology study

Figure 1a shows the transmission electron microscopy (TEM) micrograph of $BaTiO_3$ clusters. The average initial size of $BaTiO_3$ nanoparticles is around 50 nm as evidenced by TEM micrograph. The cryofractured surface morphology of PVDF/$BaTiO_3$ nanocomposites with scanning electron microscopy (SEM) is shown in Figure 1b. SEM micrograph reveals slight agglomeration of $BaTiO_3$ nanoparticles in the nanocomposites. The average aggregate size of filler in nanocomposites is around 100 nm. The microscopic observation validates the nano-dispersion of filler in the polymer matrix.

3.2. Dielectric relaxation spectroscopy (DRS) study

Dielectric spectroscopy has been widely used in polymer relaxation analysis and has the advantage over dynamic mechanical methods in that it covers much wider frequency ranges [14–17]. The study
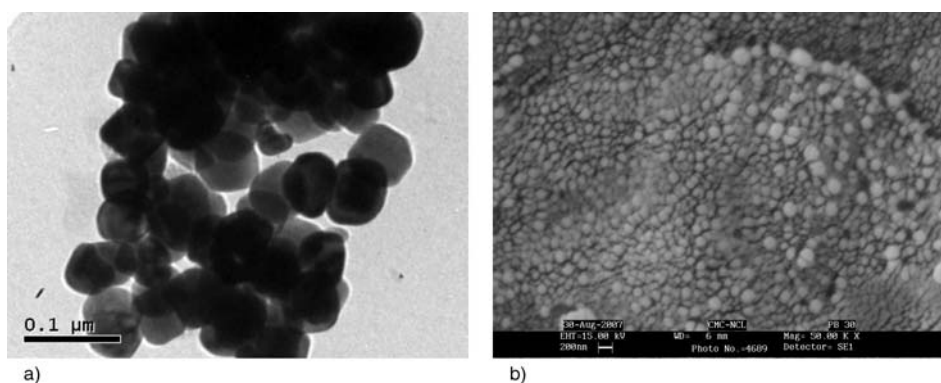
Figure 1. TEM micrograph of BaTiO₃ nanoparticles (a) and SEM micrographs of PVDF/BaTiO₃ nanocomposites with 30 wt% of BaTiO₃ nanoparticles (b)

of polymers as a function of frequency and temperature can be used to elucidate the effects due to intermolecular co-operative motions and hindered dielectric rotations.

3.2.1. Frequency dependence of dielectric constant at 30°C

Figure 2 shows the typical dielectric permittivity (ε') and dielectric loss (ε'') of PVDF/BaTiO$_3$ nanocomposites as a function of frequency at 30°C. As expected, the dielectric constant of PVDF/BaTiO$_3$ nanocomposites increases with the increase in BaTiO$_3$ content. It can be found that dielectric permittivity measured at lower frequency is always greater than higher frequency. With the increasing frequency, dielectric constant decreases very fast upto 10^{+02} Hz and in frequency range from 10^{+02} to 10^{+06} Hz it is almost constant. In the studied frequency range 10^{-02} to 10^{+07} Hz, the decrease in dielectric constant of PVDF/BaTiO$_3$ nanocomposites with increase in frequency is similar to that of PVDF. The frequency dependence of dielectric study indicates that introduction of BaTiO$_3$

Figure 2. Dielectric permittivity (ε') (a) and loss (ε'') (b) of PVDF and PVDF/BaTiO$_3$ nanocomposites as a function of frequency at 30°C

increases the dielectric constant of the PVDF from about 11 to 25 at 30 wt% of BaTiO$_3$ content.

The permittivity loss curve at 30°C shows two relaxations. The peak at 10^{+07} Hz is related to the glass transition relaxation of PVDF and is denoted as α_a relaxation [6, 8, 17, 18]. The frequency and temperature limit of instrument constraints the full view of α_a relaxation. Earlier literature work confirms peak at 10^{+07} Hz to be related to the micro-Brownian cooperative motions of the main chain backbone and is dielectric manifestation of the glass transition temperature of PVDF [19]. The relaxation peak at about 10^{+00} Hz is attributed to α_a relaxation and is associated with the molecular motions in crystalline region of PVDF. The presence of α_a relaxation peak in PVDF/BaTiO$_3$ nanocomposites explains the non-polar i.e. α phase of PVDF in nanocomposites [20]. Several interpretations of these transitions are reported [21–23]. Takahashi and Miyaji have attributed this relaxation to the reversible conformation rearrangement in the crystals while Nagakawa and Ishida have attributed this relaxation to the molecular motions in chain folds of crystalline lamellae and in the interior of crystals. Miyamoto *et al.* have ascribed this transition to the change in conformation with internal rotation that occur in crystalline phase and have reported that the defects in the crystalline phase play a major role.

3.2.2. Temperature dependence of dielectric constant

The temperature dependence of dielectric permittivity for PVDF is shown in Figure 3. As can be seen, the dielectric permittivity increases with increasing temperature. The room temperature value of permittivity at frequency 10^{-02} Hz is about 15, which increase to about 42 at 90°C. In case of permittivity loss curves, the α_a relaxation corresponding to the glass transition temperature shifts to higher frequency with increasing temperature and thus can not be detected in this experimental window, while the crystalline relaxation is clearly visible. The frequency dependence of dielectric loss can be described by Havriliak–Negami (HN) function.

Havriliak–Negami (HN) functional formalism [19] that can be phenomenologically described as a
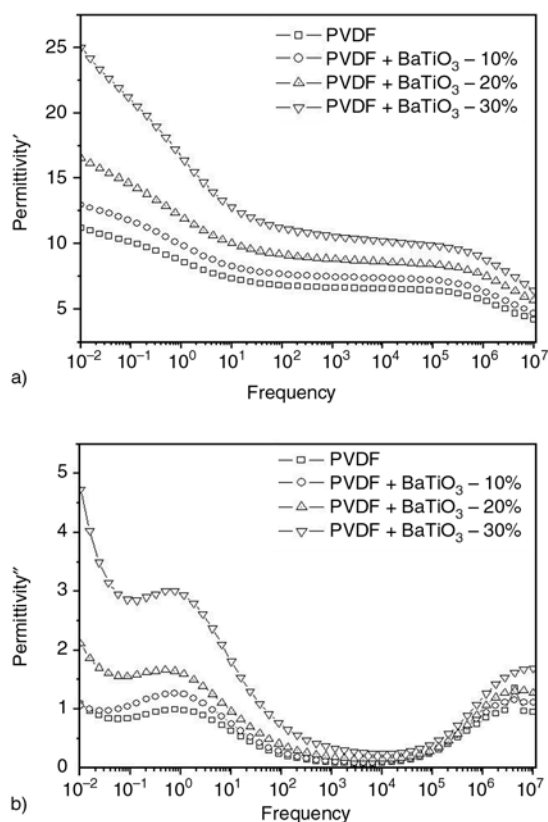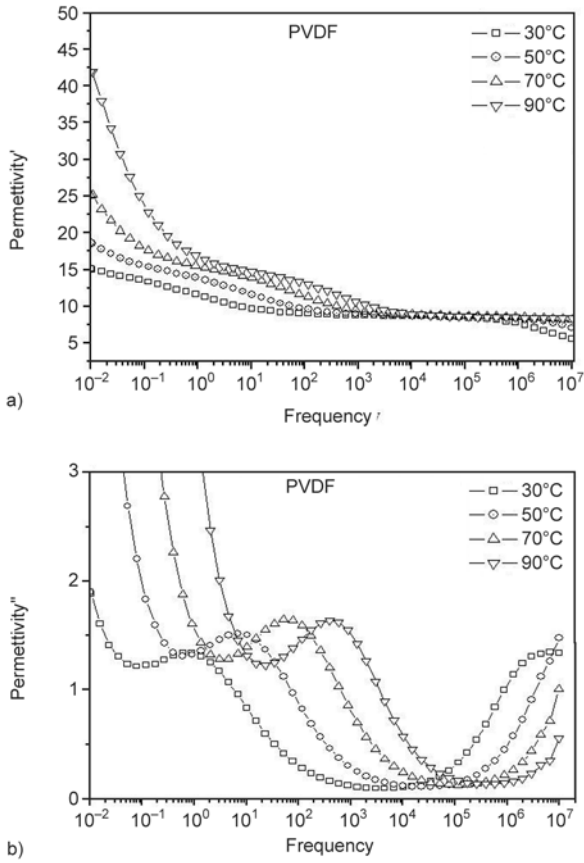
Figure 3. Dielectric permittivity (ε′) (a) and loss (ε″) (b) at various temperatures for PVDF
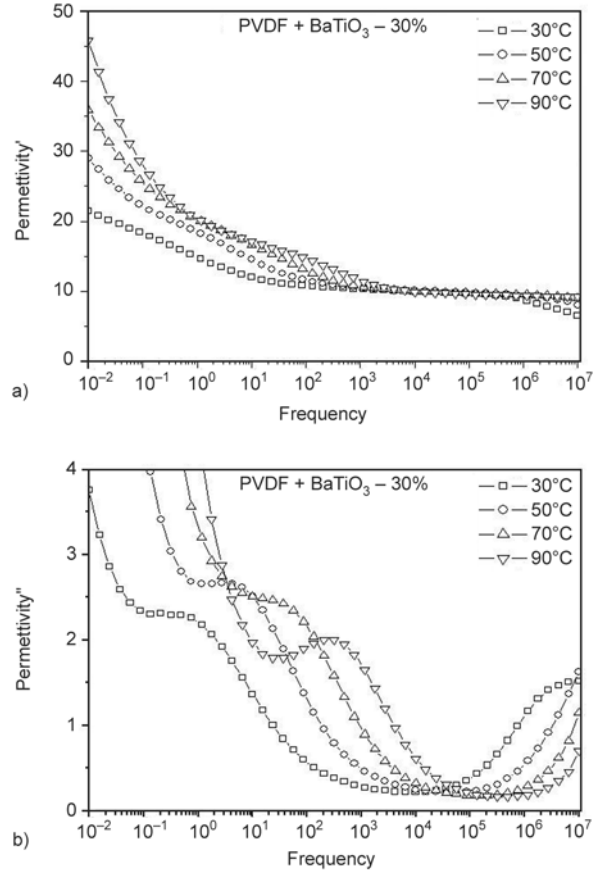
Figure 4. Dielectric permittivity (ε′) (a) and loss (ε″) (b) at various temperatures for PVDF/BaTiO$_3$ – 30%

combination of the conductivity term with the HN functional form as Equation (1):

$$\varepsilon(\omega) = \varepsilon' - i\varepsilon'' =$$

$$-i\left(\frac{\sigma_{dc}}{\varepsilon_0 \omega}\right)^N + \sum_{k=\beta,\alpha}\left[\frac{\Delta\varepsilon_k}{\left(1+(i\omega\tau_{HN\,k})^{a_k}\right)^{b_k}}\right] \quad (1)$$

where σ_{dc} is the direct current electrical conductivity, $\omega = 2\pi f$ is the angular frequency, ε_0 denotes the vacuum permittivity, N is an exponent ($0<N<1$), $\Delta\varepsilon_k$ is the dielectric of the kth process, $\tau_{HN\,k}$ is the most probable value of the central relaxation time distribution function, and a_k and b_k are shape parameters related to symmetric and asymmetric broadening of the relaxation peak, respectively. All HN fits reported here were performed using WinFit software program provided with the Novocontrol dielectric analyzer. The values of the HN parameters a and b for the nanocomposites were found to be similar to those of pure PVDF. This suggests that the intermolecular and intramolecular interac-

tions that arise in the polymer and the nanocomposites are almost identical.

PVDF/BaTiO$_3$ composites exhibit the similar dielectric behavior to that of PVDF as shown in Figure 4. However, the most apparent difference between PVDF and PVDF/BaTiO$_3$ nanocomposites can be seen at low frequency region. The conductivity effect in the low frequency is more pronounced in PVDF/BaTiO$_3$ nanocomposites as compared to that of PVDF. This behavior is similar to that observed in polyisoprene and organically modified Cloisite 25A nanocomposites [24]. The increase in the values of the permittivity and the displacement of the peak maximum of permittivity with the temperature are characteristic behavior of dielectric dispersion. Most generally, in the system with low conductivity the rapid increase of the permittivity at very low frequency is due to the electrode polarization and the effect of electrode polarization can completely masks the low frequency relaxation.

To overcome the electrode polarization effect and to resolve low frequency relaxation, 'electric mod-

ulus' formalism is used for the study of dielectric relaxations. The electric modulus formalism is introduced by McCrum *et al.* [11] and it is used to study electrical relaxation phenomena in many polymers [25–27].

The electric modulus is defined by the Equation (2):

$$M^* = \frac{1}{\varepsilon^*}, \qquad M' = \frac{\varepsilon'}{\varepsilon'^2 + \varepsilon''^2}, \qquad M'' = \frac{\varepsilon''}{\varepsilon'^2 + \varepsilon''^2}$$

(2)

where M' and M'' are the real and the imaginary part of electric modulus respectively, and ε' and ε'' are the real and the imaginary part of dielectric permittivity.

Figure 5a shows typical 3D plots of dielectric modulus spectra for pure PVDF at various temperatures as a function of frequency. Two relaxation processes can be clearly observed in the M'' curves. The relaxation peak at high frequency side is identified as fast symmetric crystalline relaxation and it shifts to higher frequency with the increasing temperature.

At high temperature, another peak appears in modulus spectra. This is attributed to Maxwell–Wagner–Sillars (MWS) polarization which can be seen in the heterogeneous materials and is also known as interfacial polarization. At temperature about 70°C the MWS relaxation peak starts appearing in PVDF whereas in PVDF/BaTiO$_3$ nanocomposites the MWS peak is seen at higher temperature about 90°C. In semicrystalline polymers, the crystalline regions are dispersed in amorphous matrix and MWS relaxation is observed in these materials due to the differences in the conductivity and permittivity values of the crystalline and amorphous phases [28, 24]. For heterogeneous composite, an interfacial polarization is almost always present because of filler additives or even impurities that migrate
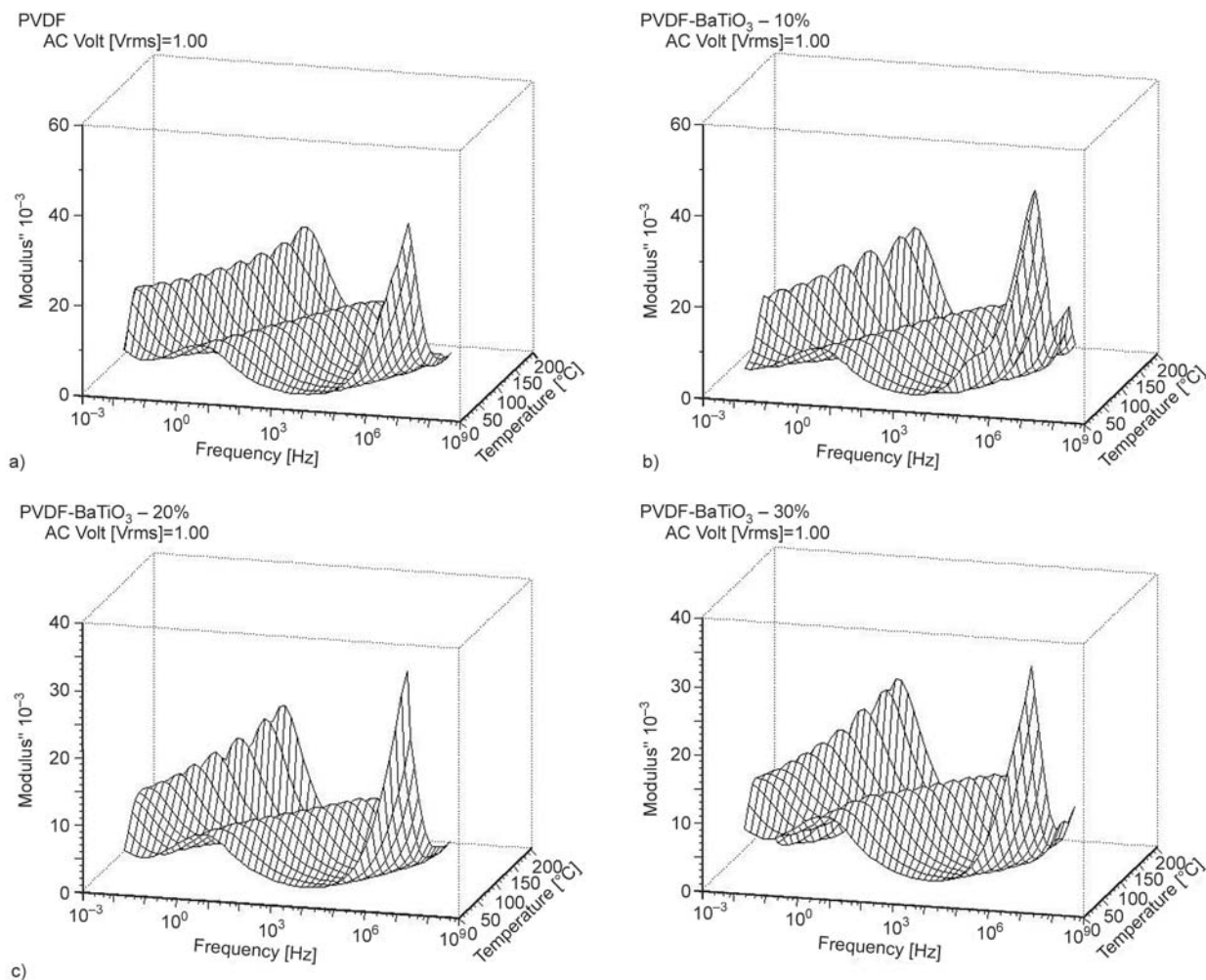
Figure 5. 3D plot of isothermal curves for PVDF (a), 3D plot of isothermal curves for PVDF/BaTiO$_3$ – 10% (b), 3D plot of isothermal curves for PVDF/BaTiO$_3$ – 20% (c), 3D plot of isothermal curves for PVDF/BaTiO$_3$ – 30% (d)

towards the interface [29]. The *M″* peaks for both relaxation processes shift to a higher frequency with increasing temperature. In addition, there is no significant change in the dielectric relaxation peak height for crystalline relaxation process, however, the intensity of dielectric relaxation peak at low frequency side increases with temperature and peak broadening decreases signifying asymmetric nature of MWS relaxation. Similar dielectric relaxation in the low frequency region below that of crystalline relaxation (α_c) is noted in earlier work on PVDF and this relaxation is ascribed to be interfacial or MWS polarization [30].

The relaxation peaks of PVDF and PVDF/BaTiO$_3$ nanocomposites as a function of frequencies at 120°C are shown in Figure 6. In case of α_c relaxation, peak appears at same frequency for polymer and nanocomposites, whereas MWS peak for PVDF/BaTiO$_3$ nanocomposites shifts to lower frequency as compared to PVDF. It can also be seen that the intensity of MWS relaxation decreases with increasing content of BaTiO$_3$ which is characteristic of MWS relaxation [31, 32]. Similar behavior is observed for PVDF/BaTiO$_3$ nanocomposites at all measured temperatures.

The temperature dependence of a relaxation process is further analyzed by plotting the frequency maximum versus reciprocal of temperature. Figure 7 shows the activation energy plots of PVDF for two relaxation processes observed. The relaxation time decreases with increasing temperature due to enhancement of mobility of charge carriers at high temperature. The temperature dependence of dielectric relaxation can be well described by the Arrhenius type behavior.
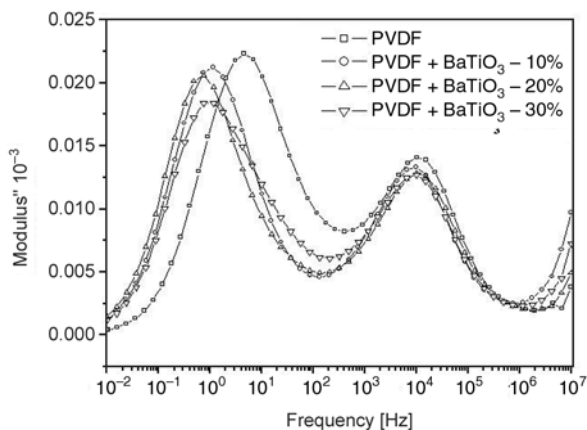
Figure 6. Comparison of dielectric modulus spectra of PVDF and PVDF/BaTiO$_3$ nanocomposite at 120°C as a function of frequency
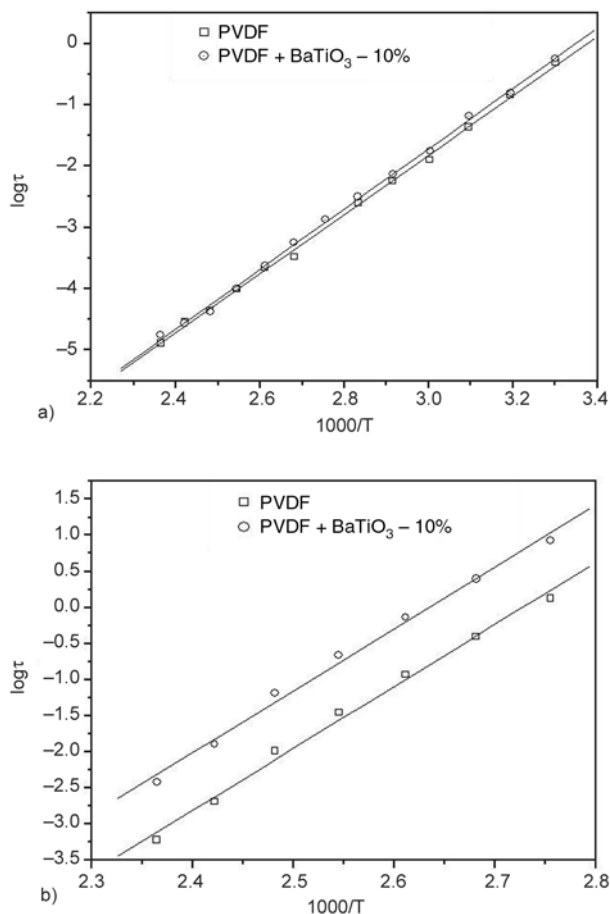
Figure 7. Activation energy plot for crystalline relaxation (a) and MWS relaxation (b) showing Arrhenius type behavior

The plot for crystalline relaxation process yields straight line and from the slope of the line activation energy can be calculated using Arrhenius equation (3):

$$f = f_0 \exp\left(-\frac{E_a}{kT}\right) \qquad (3)$$

where *f* – frequency maximum in permittivity loss spectra, E_a – activation energy, *k* – Boltzmann's constant.

The activation energy was calculated for the crystalline relaxation, α_c, for PVDF and PVDF/BaTiO$_3$ nanocomposites. The activation energy was found to be about 0.41 eV for PVDF as well as PVDF/BaTiO$_3$ nanocomposites. This value is in good agreement with the reported value of activation energy for crystalline relaxation (α_c) in PVDF [33]. The MWS relaxation shows Arrhenius type behavior indicating relaxation is thermally activated process. Table 1 summarizes the obtained results

Table 1. Fitting parameters for α_c relaxation and MWS relaxation

	α_c relaxation		MWS relaxation	
	$\log \tau$ [sec]	W [eV]	$\log \tau$ [sec]	W [eV]
PVDF	–16.41	0.42	–23.47	1.80
PVDF+BaTiO$_3$–10%	–16.32	0.41	–22.59	1.70
PVDF+BaTiO$_3$–20%	–16.22	0.41	–21.14	1.64
PVDF+BaTiO3–30%	–15.93	0.40	–20.65	1.60

for the activation energies of α_c relaxation and MWS polarization.

4. Conclusions

PVDF/BaTiO$_3$ nanocomposites are prepared using simple melt mixing technique. The BaTiO$_3$ nanoparticles are well dispersed in the PVDF matrix as evidenced by the scanning electron micrographs. The dielectric permittivity increases with increasing BaTiO$_3$ content. The room temperature dielectric spectra show two relaxations processes corresponding to the T_g and α_c relaxation while at high temperature another low frequency relaxation is observed which is attributed to the MWS relaxation. The temperature dependence of α_c relaxation and MWS relaxation follows Arrhenius type behavior. The activation energies of crystalline relaxation of MWS relaxation are not changed in nanocomposites.

Acknowledgements

References

[1] Hilczer B., Kulek J., Markiewicz E., Kosec M., Malic B.: Dielectric relaxation in ferroelectric PZT-PVDF nanocomposites. Journal of Non-Crystalline Solids, **5**, 167–173 (2002).

[2] Chiang C. K., Popielarz R.: Polymer composites with high dielectric constant. Ferroelectrics, **275**, 1–9 (2002).

[3] Kontos G. A., Soulintzis A. L., Karahaliou P. K., Psarras G. C., Georga S. N., Krontiras C. A., Pisanias M. N.: Electrical relaxation dynamics in TiO$_2$-polymer matrix composites. Express Polymer Letters, **1**, 781–789 (2007).

[4] Psarras G. C., Gatos K. G., Karahaliou P. K., Georga S. N., Krontiras C. A., Karger-Kocsis J.: Relaxation phenomena in rubber/layered silicate nanocomposites. Express Polymer Letters, **1**, 837–845 (2007).

[5] Ishida H., Campbell S., Blackwell J.: General approach to polymer nanocomposite preparation. Chemistry of Materials, **12**, 1260–1267 (2000).

[6] Gregorio R. Jr., Cestari M.: Effect of crystallization temperature on the crystalline phase content and morphology of poly (vinylidene fluoride). Journal of Polymer Science, Part B: Polymer Physics, **32**, 859–870 (1994).

[7] Pramoda K. P., Mohamed A., Phang I. Y., Liu T.: Crystal transformation and thermomechanical properties of poly (vinylidene fluoride)/clay nanocomposites. Polymer International, **54**, 226–232 (2005).

[8] Gregorio R. Jr., Ueno E. M.: Effect of crystalline phase, orientation and temperature on the dielectric properties of poly (vinylidene fluoride) (PVDF). Journal of Material Science, **34**, 4489–4500 (1999).

[9] Kremer F.: Dielectric spectroscopy: Yesterday, today and tomorrow. Journal of Non-Crystalline Solids, **305**, 1–9 (2000).

[10] Djidjelli H., Benachour D., Boukerrou A., Zefouni O., Martinez-Véga J., Farenc J., Kaci M.: Thermal, dielectric and mechanical study of poly (vinyl chloride)/olive pomace composites. Express Polymer Letters, **1**, 846–852 (2007).

[11] McCrum N. G., Read B. E., Williams G.: Anelastic and dielectric effects in polymeric solids. Wiley, London (1967).

[12] Dang Z.-M., Wang H-Y., Zhang Y-H., Qi J-Q.: Morphology and dielectric property of homogenous BaTiO$_3$/PVDF nanocomposites prepared via the natural adsorption action of nanosized BaTiO$_3$. Molecular Rapid Communications, **26**, 1185–1189 (2005).

[13] Sekar R., Tripathi A. K., Pillai P. K. C.: X-ray diffraction and dielectric studies of a BaTiO$_3$: PVDF composite. Materials Science and Engineering: B, **5**, 33–36 (1989).

[14] Madbouly S. A., Otaigbe J. U.: Broadband dielectric spectroscopy of nanostructured maleated polypropylene/polycarbonate blends prepared by in situ polymerization and compatibilization. Polymer, **48**, 4097–4107 (2007).

[15] Mijovic J., Sy J. W., Kwei T. K.: Reorientational dynamics of dipoles in poly (vinylidene fluoride)/poly (methyl methacrylate) (PVDF/PMMA) blends by dielectric spectroscopy. Macromolecules, **30**, 3042–3050 (1997).

[16] Lu H., Zhang X.: Investigation of MWS relaxation in Nylon 1010 using dielectric relaxation spectroscopy. Journal of Macromolecular Science, Part B: Physics, **45**, 933–944 (2006).

[17] Linares A., Nogales A., Rueda D. R., Ezquerra T. A.: Molecular dynamics in PVDF/PVA blends as revealed by dielectric loss spectroscopy. Journal of Polymer Science, Part B: Polymer Physics, **45**, 1653–1661 (2007).

[18] Sy J. W., Mijovic J.: Reorientational dynamics of poly(vinylidene fluoride)/poly(methyl methacrylate) blends by broad-band dielectric relaxation spectroscopy. Macromolecules, **33**, 933–946 (2000).

[19] Bello A., Laredo E., Grimau M.: Distribution of relaxation times from dielectric spectroscopy using Monte Carlo simulated annealing: Application to α-PVDF. Physical Review: B, **60**, 12764–12774 (1999).

[20] Kochervinskii V. V., Malyshkina I. A., Markin G. V., Gavrilova N. D., Bessonova N. P.: Dielectric relaxation in vinylidene fluoride-hexafluoropropylene copolymers. Journal of Applied Polymer Science, **105**, 1107–1117 (2007).

[21] Takahashi Y., Miyaji K.: Long-range order parameters of form II of poly (vinylidene fluoride) and molecular motion in the α_c relaxation. Macromolecules, **16**, 1789–1792(1983).

[22] Nakagawa K., Ishida Y.: Dielectric relaxations and molecular relaxation in poly (vinylidene fluoride) with crystal form II. Journal of Polymer Science, **11**, 1503–1533 (1973).

[23] Miyamoto Y., Miyaji H., Asai K.: Anisotropy of dielectric relaxation in crystal form II of poly (vinylidene fluoride). Journal of Polymer Science, Part B: Polymer Physics, **18**, 597–606 (1980).

[24] Mijović J., Lee H., Kenny J., Mays J.: Dynamics in polymer-silicate nanocomposites as studied by dielectric relaxation spectroscopy and dynamic mechanical spectroscopy. Macromolecules, **39**, 2172–2182 (2006).

[25] Tsangaris G. M., Psarras G. C., Kouloumbi N.: Electric modulus and interfacial polarization in composite polymeric systems. Journal of Materials Science, **33**, 2027–2037 (1998).

[26] Starkweather H. W., Avikian P.: Conductivity and the electric modulus in polymers. Journal of Polymer Science, Part B: Polymer Physics, **30**, 637–641(1992).

[27] Hodge I. M., Eisenberg A.: Conductivity relaxation in an amorphous iron containing organic polymer. Journal of Non-Crystalline Solids, **27**, 441–443 (1978).

[28] Arous M., Ben Amor I., Kallel A., Fakhfakh Z., Perrier G.: Crystallinity and dielectric relaxations in semicrystalline poly(ether ether ketone). Journal of Physics and Chemistry of Solids, **68**, 1405–1414 (2007).

[29] Psarras G. C., Manolakaki E., Tsangaris G. M.: Dielectric dispersion and ac conductivity in – iron particles loaded – polymer composites. Composites, Part A: Applied Science and Manufacturing, **34**, 1187–1198 (2003).

[30] Sasabe H., Saito S. A., Asahina M., Kakutani H.: Dielectric relaxation in poly (vinylidene fluoride). Journal of Polymer Science, Part A-2, **7**, 1405–1414 (1969).

[31] Suzhu Y., Hing P., Xiao H.: Dielectric properties of polystyrene-aluminum-nitride composites. Journal of Applied Physics, **88**, 398–405 (2000).

[32] Daly J. H., Guest M. J., Hayward D., Pethrick R. A.: The dielectric properties of polycarbonate/styrene-acrylonitrile copolymer multiplayer composites part II The Maxwell-Wagner-Sillars process. Journal of Materials Science Letters, **11**, 1271–1273 (1992).

[33] Tuncer E., Wagener M., Gerhard-Mülthaupt R.: Distribution of relaxation times in α-phase Polyvinylidene fluoride. Journal of Non-Crystalline Solids, **351**, 2917–2921 (2005).